

Received May 10, 2017; reviewed; accepted August 10, 2017

## Flotation separation of scheelite from calcite using sodium polyacrylate as depressant

Ying Zhang <sup>1,2</sup>, Rong Chen <sup>2</sup>, Youyu Li <sup>1</sup>, Yuhua Wang <sup>3</sup>, Ximei Luo <sup>2,3</sup>

<sup>1</sup> State Key Laboratory of Complex Nonferrous Metal Resources Clean Utilization, Kunming 650093, China

<sup>2</sup> Mineral Processing Engineering, Faculty of Land Resource Engineering, Kunming University of Science and Technology, Kunming 650093, China

<sup>3</sup> Mineral Processing Engineering, School of Minerals Processing and Bio-engineering, Central South University, Changsha 410083, China

Corresponding authors: zhyingcsu@163.com (Ying Zhang), wangyh@mail.csu.edu.cn (Yuhua Wang)

**Abstract:** The depressing properties of sodium polyacrylate (PA-Na) for calcite from scheelite were studied by microflotation experiments, zeta potentials, X-ray photoelectron spectroscopy (XPS) and density functional theory (DFT) calculation. Flotation results revealed that the selective depression effect of PA-Na was better than that of sodium silicate ( $\text{Na}_2\text{SiO}_3$ ), and PA-Na can depress calcite more effectively than scheelite. The flotation recovery of scheelite and calcite kept at about 75% and 15% respectively at the pulp pH 9.3~9.6 and PA-Na concentration from 37.5 mg/dm<sup>3</sup> to 50 mg/dm<sup>3</sup>. The zeta potentials of the minerals were significantly altered and the zeta potential of calcite became more negative than scheelite. XPS analysis deduced the occurrence of chemisorption between PA-Na and mineral surfaces, and the chemisorption of PA-Na on calcite was stronger than on scheelite. The results from DFT calculation demonstrated that the absolute value of the adsorption energy in the presence of PA-Na on the surface of calcite {104} was larger than on the surface of scheelite {111}. With the combination of the analysis, it could be concluded that calcite was more easily depressed than scheelite, and this finding remarkably matched with the microflotation experimental results. Furthermore, by using PA-Na as depressant, the flotation separation of scheelite from calcite can be achieved by controlling the flotation pH and PA-Na dosage.

**Keywords:** scheelite, calcite, flotation, sodium polyacrylate, selective depression

### 1. Introduction

Calcium-bearing minerals such as scheelite, calcite are important industrial minerals, they can be used as raw materials for production of spaceflight, cement and so on. But the separation of scheelite and calcite is a difficult issue in flotation, which is the common method to separate them. However, the difficulty of flotation of scheelite from calcite is due to the existence of the same cation in the minerals surface and similar physicochemical characteristics such as solubility, hardness, specific gravity and PZC (point of zero charge) (Gao et al., 2016). The Petrov method (Lii et al., 1983) is the conventional way for scheelite flotation, which is operated at the condition of high temperature, high concentrate pulp, strongly stirring, high pH and high dosage of sodium silicate. The harsh flotation process conditions cause a high operation cost (Gao et al., 2010). At room temperature, a reagent called 731 (oxidized paraffin soap) could be used as collector for scheelite (Liu et al., 2016), and high enrichment ratio could be achieved in rougher flotation. But in this process a large amount of sodium silicate is needed to be added to the pulp (Gao et al., 2016; Feng et al., 2015). Recently, the flotation with lime addition was studied (Liu et al., 2013). The carrier flotation (Qiu, 1983) and shear flocculation flotation (Kohl et al., 1986) were reported as new technologies for scheelite flotation. In order to make the separate of scheelite from calcite effectively and economic effectively, a more effective depressant,

which can be used under normal flotation conditions, is need. In this regard, a research programme was carried out by using polyacrylate as depressant for flotation of scheelite from calcite.

PA-Na is a water-soluble linear polymer. High-molecular-weight PA-Na can be used as flocculant (Wang et al., 2008; Huang et al., 2008), whereas the low-molecular-weight form can be employed as depressant, dispersant (Rubio et al., 1987) or water-treatment agent (Guerrero et al., 1987). PA-Na is effective only in the flotation of some special kinds of sulphide and oxide ores, such as lead-zinc sulphide (Silvestre et al., 2009), refractory copper oxide (Yang et al., 2000) and lead-zinc oxide ores.

PA-Na is a complex of polyelectrolyte particles and can dissociate into low-molecular-weight ions ( $\text{Na}^+$ ) and polymer ions when the compound is dissolved in an aqueous solution. The polymer ions containing numerous carboxylate ions are multivalent ions. PA-Na is commonly known as depress materials by forming a water-soluble complex with the calcium ions ( $\text{Ca}^{2+}$ ) in the surfaces of mineral (Bulatovic, 2007). The complex would sink to the underflow and rely on the advantages of large quantities of PA-Na, thereby reducing the influence of mineral floatability on collector addition. In this regard, PA-Na could be a depressant for calcite during the flotation of scheelite.

In this paper, the flotation response of scheelite and calcite were evaluated by microflotation experiments with/without addition of PA-Na or  $\text{Na}_2\text{SiO}_3$  as depressant. Attempt was made to understand the mechanism of selective depress of calcite during the flotation of scheelite by using Zeta potential measurement, X-ray photoelectron spectroscopy (XPS) analysis. In addition, the adsorption energy of PA-Na on scheelite {111} surface and calcite {104} surface was calculated using the density functional theory (DFT).

## 2. Material and methods

### 2.1 Materials

Pure scheelite was obtained from Ke Muda Mining Ltd. in Tongde County, Qinghai Province, China, and pure calcite was obtained from a mineral powder factory in Changsha, Hunan Province, China. The samples were firstly handpicked, crushed, ground, screened and finally stored in sealed glass bottles. Elemental analysis showed that the purity of the scheelite and calcite samples were 94% and 98%, respectively. The particle-size distributions of the samples are displayed in Table 1. The ground samples were wet-sieved, and -74  $\mu\text{m}$  sized fractions with specific surface areas of 2533.03  $\text{cm}^2/\text{g}$  for scheelite and 2596.77  $\text{cm}^2/\text{g}$  for calcite were collected and used in micro flotation experiments. Some of these particle fractions were further ground in agate mortar to obtain -2  $\mu\text{m}$  particles for zeta potential measurements and XPS analysis.

Table 1. Particle size distribution of the samples

Samples	$X_{10}$	$X_{16}$	$X_{50}$	$X_{84}$	$X_{90}$	$X_{99}$	SMD	VMD
Scheelite	2.61	4.47	31.14	81.15	95.17	143.44	7.79	40.98
Calcite	3.05	5.14	17.19	52.39	66.73	121.9	7.60	27.04

SMD: the average diameter of the surface

VMD: the volume average diameter

PA-Na (analytical-reagent grade; Tianjin Kermel Chemical Reagent Co., Ltd.) was used as depressant to depress calcite selectively; its molecular weight ranges from 800 million g/mol to 1000 million g/mol.  $\text{Na}_2\text{SiO}_3$  (Yin et al., 2015) (analytical-reagent grade; Tianjin Dingshengxin Chemical Industry Co., Ltd.) is the active ingredients of water glass which is a conventional depressant for scheelite flotation. The collector was a sodium soap of fatty acids formulated from oxidised paraffin (731), which is an industrial-grade product and is widely applied in scheelite flotation. Sodium carbonate and hydrochloric acid (Tian-heng Chemicals) were used to adjust the pH of the pulp. Distilled water was utilized in all the experiments.

### 2.2 Flotation experiments

Flotation experiments were carried out in a self-priming trough flotation machine (Fig. 1, Jilin Prospecting Machinery Factory, Changchun, China). The volume of the cell is 40  $\text{cm}^3$ , and the

rotational speed in the cell is 1650 rpm during flotation. The flotation was conducted as a function of pH in the absence and presence of PA-Na or  $\text{Na}_2\text{SiO}_3$ . The mineral suspension was prepared by adding 3 g of minerals to 40  $\text{cm}^3$  of solutions. During the experiments, the pH of the pulp was adjusted to a desired value by adding  $\text{Na}_2\text{CO}_3$  or HCl stock solutions for 2 min, which was measured with pH meter. The prepared depressant and 731 were added at a desired concentration and conditioned for 3 min. During each flotation experiment, the froth was collected for 3 min. The dry weights of the concentrate and tail were measured and used to calculate the recovery. Each microflotation experiment was measured three times, and the average was reported as the final value. The standard deviation, which is presented as an error bar, was obtained using the mean of the three measurements per experimental condition. The flotation flowsheet of the pure minerals is shown in Fig. 2.



Fig. 1. Scheme of flotation machine

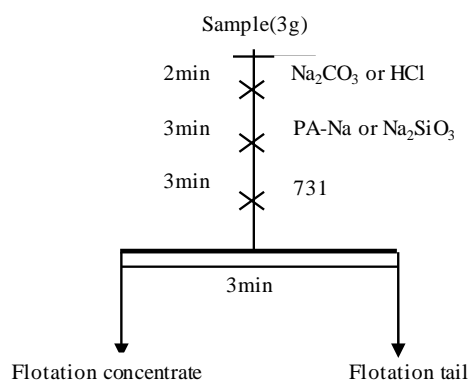


Fig. 2. Flotation flowsheet of pure minerals

### 2.3 Zeta potential measurements

Isoelectric points (iep) of mineral samples were determined by measuring the electrophoretic mobility of aqueous dispersions as a function of pH in a zeta potential meter (Delsa 440SX, Beckman Coulter Company, Brea, CA, USA). For these measurements, a mineral dilution suspension was prepared by adding 0.03 g mineral to 50  $\text{cm}^3$  of  $10^{-3}$  M potassium nitrate solution and ultrasonicated for 3 min, and then magnetically stirred for 10 min. The pH was adjusted using  $\text{Na}_2\text{CO}_3$  or HCl.

### 2.4 XPS analysis

The XPS tests were performed using a K-Alpha 1063 spectrometer (Thermo Fisher Scientific, Chanhassen, MN, USA) with an Al  $K_{\alpha}$  emission for the X-ray source (operating at 72W). A double-gathered and hemi-spherical analyser was employed, with the angle of the sample surface to the analyzer set to  $180^{\circ}$ . The diameter of the beam spot was 400  $\mu\text{m}$ . The analyzer involved a 128-channel detector with an energy resolution better than 0.5 eV and an error value of 0.3 eV. Samples were mounted on the holder with double-sided tape and transferred to the analysis chamber, in which the vacuum was  $10^{-9}$  mBar. XPS spectra were obtained at room temperature by using PA-Na as

depressant. The C 1s value of 284.8 eV was selected as the reference line. Thermo Avantage software was employed to analyse the XPS data (Sun et al., 2013).

Samples were prepared by adding 1.0 g of pure mineral ( $< 2 \mu\text{m}$ ) and a moderate amount of distilled water in a hitch groove at an effective volume of approximately  $40 \text{ cm}^3$ . In accordance with the single-mineral flotation process, we added the reagents, conditioned the mixture for 30 min and then allowed the mixture to stand for another 30 min. The mixture was subsequently centrifuged for solid-liquid separation, and the sunken fractions were washed twice to thrice with distilled water and then dried in a vacuum oven. Afterwards, the samples were subjected to XPS analysis.

## 2.5 Computational details

This study also investigated the competitive adsorption of PA-Na and water on the mineral surface (Cooper et al., 2004). The surface energy ( $E_M$ ) of the mineral surface was  $-37510.89 \text{ eV}$ . The adsorption energy of the adsorbate at the mineral surface was calculated using Eq. 1:

$$E_{ads} = E_{M+R} - (E_M + E_R), \quad (1)$$

where  $E_{M+R}$  is the energy of the mineral surface with adsorbate PA-Na or water molecules,  $E_M$  is the energy of the mineral surface; and  $E_R$  is the self-energy of the free adsorbate molecule, which is calculated using the same simulation parameters.

In an aqueous environment, the adsorption of PA-Na on the mineral surface was achieved by displacing the pre-adsorbed water on the mineral surface. Consequently, we compared the adsorption energy of PA-Na or water at different modes of adsorption. A negative and lower adsorption energy indicates that PA-Na is more easily overcomes the resistance of the pre-adsorbed water on the mineral surface. The lowest value was selected for the final evaluation.

Accordingly, in the aqueous environment the adsorption energy of mineral surface was given by (Leeuw et al., 2003; Pradip et al., 2002)

$$E_{ads} = E_a - E_b, \quad (2)$$

where  $E_{abs}$  is the final value of adsorption energy. A more negative value of  $E_{abs}$  indicates that the adsorption reaction of PA-Na occurs more easily. Specifically,  $E_a$  is the adsorption energy of the PA-Na molecule on the mineral surface, and  $E_b$  is the adsorption energy of the water molecule on the mineral surface.

The adsorption energy of the adsorbate molecule was calculated using the Cambridge Sequential Total Energy Package (CASTEP) (Payne et al., 1992; Zhao et al., 2013). In the CASTEP module, Ultrasoft pseudopotentials were used to represent the interactions between the adsorbate and the minerals. The exchange-correlation energy was determined by a generalised gradient approximation of Perdew-Burke-Ernzerhof (GGA-PBE) (Perdew et al., 1996). Reciprocal space integration over the Brillouin zone was approximated with finite sampling of the  $k$ -point by using the Monkhorst-Pack scheme, and the  $k$ -point spacing was set to  $0.04 \text{ \AA}^{-1}$ . The atomic coordinates were optimised using a Broyden-Fletcher-Goldfarb-Shanno scheme, which utilises the total energy and the Hellmann-Feynman forces ( $< 0.05 \text{ GPa}$ ) on the atoms. The scheme adopted the following thresholds for the converged structure: (a) energy tolerance of  $1.0 \times 10^{-5} \text{ eV/\AA}$ , (b) maximum force tolerance of  $0.03 \text{ eV/\AA}$  and (c) maximum displacement tolerance of  $0.001 \text{ \AA}$  (Gao et al., 2013).

## 3. Results and discussion

### 3.1 Single-mineral flotation

To compare PA-Na with conventional depressant  $\text{Na}_2\text{SiO}_3$ , single-mineral flotation of scheelite and calcite were carried out as a function of pH in the absence and presence of PA-Na or  $\text{Na}_2\text{SiO}_3$  (Fig. 3). The usages of PA-Na and  $\text{Na}_2\text{SiO}_3$  were  $25 \text{ mg/dm}^3$  and  $500 \text{ mg/dm}^3$ , respectively. The usage of 731 was  $75 \text{ mg/dm}^3$ , which was used as collector. The recovery of scheelite and calcite were almost unchanged in the absence of depressant. With  $\text{Na}_2\text{SiO}_3$  as depressant, the recovery of scheelite and calcite had stable responded all pH range.  $\text{Na}_2\text{SiO}_3$  had little depressant effect on scheelite and calcite. By contrast, in the presence of PA-Na, the flotation recovery of scheelite and calcite increased as the pH increases and then decreased. However, the pH values at the maximum recovery for scheelite and calcite were different. The experimental results of scheelite are similar to those reported by Feng et al.

(2015). With PA-Na as depressant, the scheelite floated well with a recovery of about 80%, which was obtained over a wide pH range of 8.7 to 10. By contrast, PA-Na had a significant depressing effect for calcite, and the maximum recovery of calcite was 45.58% at pH 8.01. In short, the single-mineral flotation results showed PA-Na had a more preferential than  $\text{Na}_2\text{SiO}_3$  for flotation separation scheelite from calcite at pulp pH between 7.5 and 10.5.

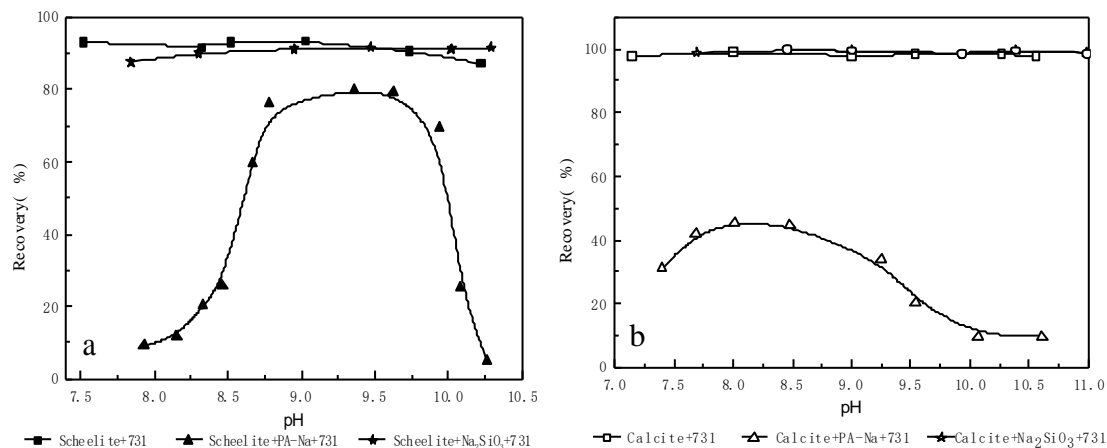


Fig. 3. Flotation recovery of scheelite and calcite as a function of pH in absence and presence of PA-Na or  $\text{Na}_2\text{SiO}_3$

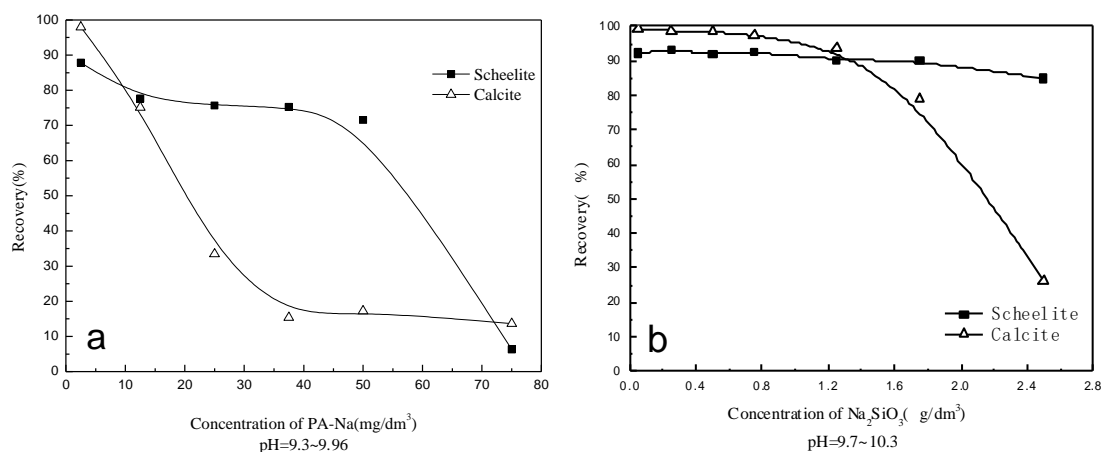


Fig. 4. Flotation recovery of scheelite and calcite as a function of concentration of PA-Na or  $\text{Na}_2\text{SiO}_3$

As the PA-Na or  $\text{Na}_2\text{SiO}_3$  concentration increasing, at the suitable pulp pH the flotation recoveries of scheelite and calcite are shown in Fig. 4, while the usage of 731 was  $75 \text{ mg/dm}^3$ . The results of Fig. 4(a) show the effect of PA-Na concentration on the recovery of scheelite at the pH 9.3~9.6. The scheelite is floated well with a recovery greater than 71.57%, which is obtained over a wide PA-Na concentration range less than  $50 \text{ mg/dm}^3$ . When the PA-Na concentration exceeded  $50 \text{ mg/dm}^3$ , the flotation recovery of scheelite decrease sharply. The flotation recovery of calcite decline significantly as the PA-Na concentration increase to  $37.5 \text{ mg/dm}^3$ . When the PA-Na concentration exceeded  $37.5 \text{ mg/dm}^3$ , the flotation recovery of calcite stabilised at about 15%. The effect of  $\text{Na}_2\text{SiO}_3$  concentration on the recovery of calcite at the pH 9.7~10.3 is shown in Fig. 4(b). With the increase of  $\text{Na}_2\text{SiO}_3$  concentration from  $0.05 \text{ g/dm}^3$  to  $1.25 \text{ g/dm}^3$ , the reduction of scheelite and calcite recovery is very small. When the  $\text{Na}_2\text{SiO}_3$  concentration increase from  $1.25 \text{ g/dm}^3$  to  $2.5 \text{ g/dm}^3$  the recovery of scheelite is decreased by 5.27%, but the recovery of calcite is decreased from 93.4% to 26.25%. Scheelite and calcite separation could be achieved by flotation with  $2.5 \text{ g/dm}^3$  of  $\text{Na}_2\text{SiO}_3$  addition at the pH 9.7~10.3. In general, the flotation separation using of PA-Na as depressant is better than using  $\text{Na}_2\text{SiO}_3$  regarding to dosage and pH. The flotation separation of scheelite and calcite can be achieved, while

the pulp pH is between 8.7 and 10 and PA-Na concentration is between 37.5 and 50 mg/dm<sup>3</sup> (Figs. 3 and 4).

### 3.2 Zeta potential measurements

Zeta potential measurement is an in-situ method used to explore the interactions of ionic species with minerals. In this research, the zeta potentials of scheelite and calcite pulp were measured in absence and presence of PA-Na. The pH modifiers were hydrochloric acid and sodium carbonate. The measured zeta potentials for scheelite and calcite are shown in Figs. 5 and 6, respectively.

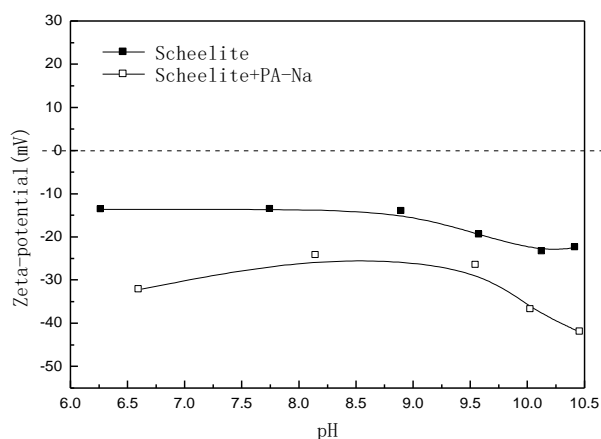


Fig. 5. Zeta-potential of scheelite as a function of pH in absence and presence of PA-Na

The trends of the zeta potential of scheelite as a function of pH in absence and presence of PA-Na are shown in Fig. 5. Without PA-Na addition (solid symbols), the  $pH_{IEP}$  of scheelite do not lie in the pH range of 6 and 10.5, which is in accordance with previous reports (Gao et al., 2015). The zeta potential is negative and values range is between -13 mV and -24 mV, similar to the results reported by Gao et al. (2016). With addition of 25 mg/dm<sup>3</sup> PA-Na the scheelite surface potential shifts to more negative direction over the testing pH range. This effect is considered responsible for the adsorbing of negatively charged COO<sup>-</sup> anions on the negatively charged mineral surface.

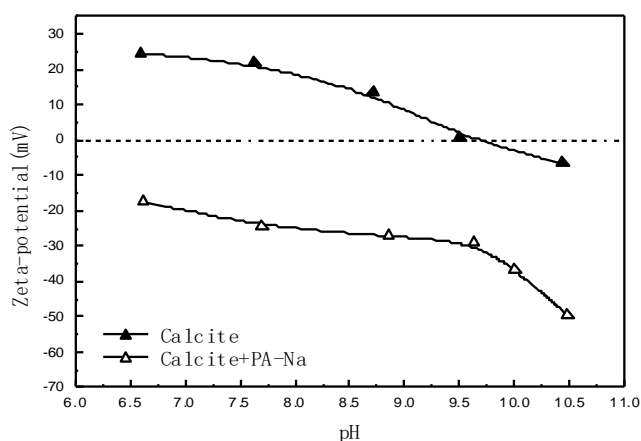


Fig. 6. Zeta-potential of calcite as a function of pH in absence and presence of PA-Na

As shown in Fig. 6, it displays the zeta potential of calcite as a function of pH in absence and presence of PA-Na. The  $pH_{IEP}$  of calcite was 9.5 without addition of PA-Na (solid symbols). The  $pH_{IEP}$  of calcite is similar to this reported by Gao et al. (2015). The addition of 37.5 mg/dm<sup>3</sup> PA-Na caused a significant shift of the Zeta-potential with the pH range between 6 and 10.5. Such significant shift in Zeta-potential infers a strong interaction of PA-Na with calcite, which was caused by adsorption possibly. Potentiometric titration results (Drzymala et al., 1981) show that PA-Na is not dissociated at pH < 4, the COO<sup>-</sup> in the PA-Na are partially dissociated at neutral pH, but it is dissociated fully at pH

> 9.5. So, it is presumed that the COO<sup>-</sup> is dissociated basically at pH > 9, the molecular chain stretching makes a large number of COO<sup>-</sup> absorbed on the calcite surface. PA-Na addition exerts stronger influence on the zeta potentials of calcite than those of scheelite over the pH range studied, which indicates there is a much stronger adsorption of PA-Na on calcite than on scheelite (Figs. 5 and 6). Therefore, PA-Na has better depressing effect and higher selectivity for calcite. This observation corresponded well with the flotation results which indicated that the floatability of calcite was much weaker than that of scheelite in presence of PA-Na (Fig. 3).

### 3.3 XPS results

The atomic compositions of scheelite and calcite interfaces before and after PA-Na treatment are listed in Table 2. After PA-Na adsorption, the Ca, C and O atomic concentration of scheelite increased 0.26%, 0.37% and 0.49% respectively, that of W decreased 1.12%; the atomic concentration of Ca and C of calcite decreased 0.25% and 12.26%, that of O increased 12.51%. It confirmed there was adsorption of PA-Na on the two mineral surfaces. In the process of dissolution, scheelite and calcite will produce a lot of Ca<sup>2+</sup> ions (Wang et al., 1988). The reason maybe that Ca<sup>2+</sup> ion react with PA-Na to form calcium polyacrylate which can cover on the surface of the mineral, so that the concentration of calcium atoms on the mineral surface increases (Ylikantola et al., 2013). The results in Table 2 also indicate that the change values of atomic concentration for C and O atoms on calcite interface were far greater than those on scheelite interface, which inferred that the adsorption capacity of PA-Na on calcite was higher than that on scheelite.

Table 2. Atomic concentration of elements for mineral interfaces as determined by XPS

Samples	Atomic concentration of elements (atomic %)			
	Ca	W	C	O
Scheelite	11.33	18.55	26.96	43.16
Scheelite+PA-Na	11.59	17.43	27.33	43.65
$\Delta^a$	0.26	-1.12	0.37	0.49
Calcite	19.72	<sup>b</sup>	39.84	40.44
Calcite +PA-Na	19.47	<sup>b</sup>	27.58	52.95
$\Delta^a$	-0.25	<sup>b</sup>	-12.26	12.51

<sup>a</sup>  $\Delta$  Is defined as the value of post-treatment minus the value of pre-treatment by PA-Na.

<sup>b</sup> Is defined as none.

The Ca2p, W4f, C1s or O1s XPS of scheelite and calcite before and after PA-Na treatment were listed in Fig. 7 and Fig. 8. The results in Fig. 7 illustrated that the changes in the peak intensities of Ca2p<sub>3/2</sub>, Ca2p<sub>1/2</sub> and W4f may be induced by PA-Na addition. In the Ca2p<sub>3/2</sub> and Ca2p<sub>1/2</sub> spectra, the binding energies of scheelite were 346.82 eV and 350.28 eV, respectively. After PA-Na addition, the peak position of Ca2p shifted toward a higher binding energy; the binding energies of scheelite increased to 346.85 eV and 350.38 eV, correspondingly. The binding energies shifted by 0.03 eV and 0.1 eV, respectively (Fig. 7(a)). These findings indicated the presence of a weak force of interaction between the scheelite surface and PA-Na. In the W4f spectra, the binding energies shifted by 0.1 eV and 0.01eV respectively, which was less than the experimental error of 0.3 eV (Fig. 7(b)). Thus, PA-Na did not influence the Ca2p<sub>3/2</sub>, Ca2p<sub>1/2</sub> and W4f of the inner electron binding energies of scheelite.

The XPS patterns of calcite (Fig. 8) significantly changed after the addition of PA-Na. Fig. 8 presented the binding energies of the elements in calcite before and after reacting with PA-Na, and these findings suggested that the changes in the peak intensities of Ca2p<sub>3/2</sub>, Ca2p<sub>1/2</sub>, C1s and O1s were induced by PA-Na addition. The binding energy of the Ca2p<sub>3/2</sub> peak increased from 346.48 eV to 347.18 eV, and the binding energy of the Ca2p<sub>1/2</sub> peak also increased from 350.08 eV to 350.88 eV, showing chemical shifts of 0.7 and 0.8 eV, correspondingly, which was relative to the binding energies before PA-Na addition (Fig. 8(a)). When the shift is greater than the experimental error of 0.3 eV, it indicates that a chemical reaction occurs, the greater of the chemical shift, the stronger of the reaction (Moreira et al., 2017; Parasyuk et al., 2017). The increase in the binding energy of the calcite surface

after PA-Na addition implied the existence of a strong force of adsorption on calcite. In the C1s spectra, the chemical shift of the binding energy was 0.45 eV (Fig. 8(b)). In the O1s spectra, the chemical shift of the binding energy was 0.7 eV (Fig. 8(c)). Thus, PA-Na significantly affected the binding energies of Ca2p, C1s and O1s on the calcite interface.

In summary, the XPS tests showed that the chemical shift of PA-Na is in the order of scheelite << calcite, suggesting the stronger adsorption PA-Na on calcite than on scheelite. This finding correlated well with the results of the microflotation experiments.

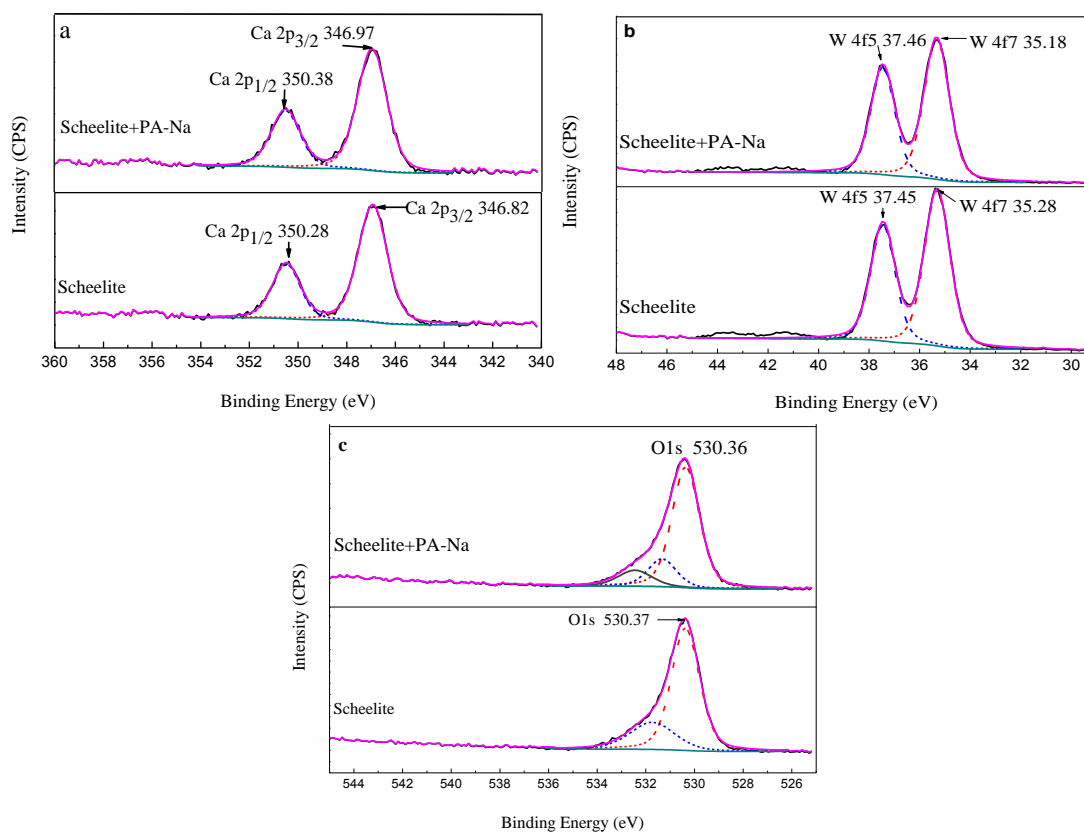


Fig. 7. Ca2p, W4f or O1s of scheelite before and after PA-Na treatment: (a) Ca2p of scheelite, (b) W4f of scheelite, (c) O1s of scheelite

### 3.4 Adsorption energy

The modes of adsorbate molecule interaction on scheelite {111} surface and calcite {104} surface significantly affected the results of the quantum chemical method. The mineral crystal structure and basic unit structure of PA-Na and water were built in a crystal builder module (Hu et al., 2012; Zhang et al., 2014). According to the research reports, the magnitude of the adsorption energy can be determined by the form of adsorption (Hu et al., 2016). In other words, if the adsorption is negative, indicating that the adsorption process is exothermic process, and the adsorption is stable. The greater the absolute value of the adsorption, the stronger the reaction (Yang et al., 2017; Deng et al., 2015). The modes of PA-Na adsorption on the scheelite {111} surface included the adsorption of the calcium atoms on different electron shells (WP1) and on the same electron shell (WP2). The modes of H<sub>2</sub>O adsorption on the scheelite {111} surface involved adsorption on the top of the oxygen atom (WH1), on the two oxygen atoms of a single tungstate group (WH2) and on the two oxygen atoms from different tungstate groups (WH3).

A detailed description of the comparison between the sorption of PA-Na and the pre-adsorbed water are presented in Tables 3 and 4. Table 3 provided the adsorption energies of the adsorbates on the scheelite {111} surface. The adsorption energy of the mode of WP2 was -359.27 kJ/mol, which was lower than that of mode of WP1. These results denoted that the adsorption between PA-Na and the scheelite {111} surface involved chemisorption. The adsorption energy of the water molecules was the



lowest at the mode of WH2, the energy value was -225.70 kJ/mol, which was indicated a strong adsorption between the water molecules and the scheelite {111} surface.

The mode of PA-Na adsorption on the calcite {104} surface included the adsorption of calcium atoms on x-axis (CP1) and on y-axis (CP2). The mode of H<sub>2</sub>O adsorption on the calcite {104} surface involved the adsorption on the top of the oxygen atom (CH1), on the two oxygen atoms of a single carbonate group (CH2) and on the two oxygen atoms from different carbonate groups (CH3).

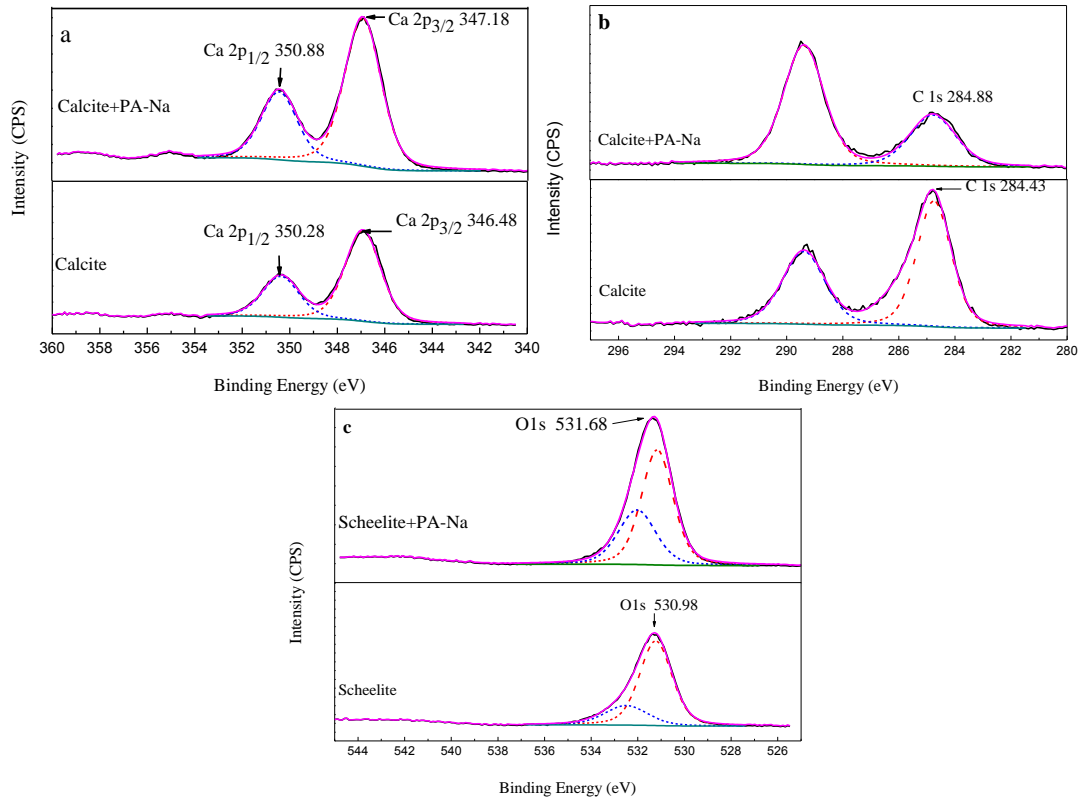


Fig. 8. Ca2p, C1s and O1s of calcite before and after PA-Na treatment: (a) Ca2p, (b) C1s, (c) O1s

Table 3. Adsorption energy of PA-Na and water on scheelite {111} surface

Mineral	Mode of adsorption	$E_{(M+R)}$ (eV)	$E_M$ (eV)	$E_R$ (eV)	$E_{ads}$ (eV)	$E_{ads}$ (KJ/mol)
Scheelite	WP1	-42915.93	-37510.89	-5401.65	-3.39	-327.21
+PA-Na	WP2	-42916.26	-37510.89	-5401.65	-3.76	-359.27
Scheelite	WH1	-37978.42	-37510.89	-467.20	-0.32	-31.27
+ H <sub>2</sub> O	WH2	-37980.43	-37510.89	-467.20	-2.34	-225.70
	WH3	-37979.35	-37510.89	-467.20	-2.26	-121.50

The adsorption energy of PA-Na on the calcite {104} surface was shown in Table 4. The adsorption energy of PA-Na was -289.06 kJ/mol at the mode of CP1, which was lower than the mode of CP2. This finding demonstrated that the adsorption between PA-Na and the calcite {104} surface involved chemisorption. The adsorption energy of the water molecules was the lowest at the mode of CH2, the the energy value was -110.52 kJ/mol, indicating a strong adsorption between the water molecules and the calcite {104} surface.

The adsorption energy of PA-Na in an aqueous environment was calculated using Eq. 2, and the results were listed in Table 5. The results for  $E_{abs}$  were negative, and the adsorption energy of PA-Na on calcite in the aqueous environment was lower than that on scheelite, confirming that PA-Na exhibited better selectivity for calcite than scheelite. This finding was consistent with the results of the microflotation experiments.

Table 4. Adsorption energy of PA-Na and water on calcite {104} surface

Mineral	Mode of adsorption	$E_{(M+R)}$ (eV)	$E_M$ (eV)	$E_R$ (eV)	$E_{ads}$ (eV)	$E_{ads}$ (KJ/mol)
Calcite	CP1	-74544.88	-69140.48	-5401.40	-3.00	-289.06
+PA-Na	CP2	-74543.77	-69140.48	-5401.40	-1.88	-181.17
Calcite	CH1	-69608.01	-69140.48	-467.06	-0.47	-45.01
+ H <sub>2</sub> O	CH2	-69608.69	-69140.48	-467.06	-1.15	-110.52
	CH3	-69608.24	-69140.48	-467.06	-0.70	-67.07

Table 5. The adsorption energy of PA-Na adsorbing on the scheelite {111} surface and calcite {104} surface in aqueous environment (KJ/mol)

Mode of adsorption	$E_b$	Mode of adsorption	$E_a$	$E_{ads}$
Scheelite+H <sub>2</sub> O	-225.70	Scheelite + PA-Na	-359.27	-133.57
Calcite+H <sub>2</sub> O	-110.52	Calcite + PA-Na	-289.06	-178.54

#### 4. Summary and conclusions

In this paper, PA-Na was used as a depressant for selective depression calcite from scheelite. The flotation performance and mechanism for separation calcite from scheelite were evaluated by microflotation experiments, Zeta potential measurement, XPS analysis and DFT calculation. Based on the experimental results, the following conclusions can be drawn:

The microflotation results demonstrated that the selective depression of PA-Na was stronger than that of Na<sub>2</sub>SiO<sub>3</sub>. PA-Na exhibited superior depressing performance for calcite and a weak depressing for scheelite. With the use of PA-Na as a depressant at its optimum concentration ranged from 37.5 mg/dm<sup>3</sup> to 50 mg/dm<sup>3</sup>, scheelite can be floated well over a pulp pH range between 8.7 and 10, whereas calcite can be depressed at the same pH values.

The results of zeta potential, XPS and DFT calculation illustrated there was a stronger chemisorption of PA-Na on calcite than on scheelite. The PA-Na addition showed more distinct electrokinetics in calcite than in scheelite. In the aqueous environment, the absolute value of adsorption energy of PA-Na on calcite was higher than that on scheelite, confirming that PA-Na exhibited better selectivity for calcite than for scheelite. This investigation of mechanism was consistent with the results of the microflotation experiments.

#### Acknowledgements

This study was financially supported by the National Natural Science Foundation of China (No. 51504108 and No. 51604130).

#### References

- BULATOVIC S.M., 2007. *Handbook of Flotation Reagents: Chemistry Theory and Practice*. Amsterdam: Elsevier Science & Technology, 25.
- COOPER T.G., LEEUW N.H., 2004. *A computer modelling study of the competitive adsorption of water and organic surfactants at the surfaces of the mineral scheelite*. *Langmuir*, 20 (10), 3984-3994.
- DENG J.S., LEI Y.H., WEN S.M., CHEN Z.X., 2015. *Modeling interactions between ethyl xanthate and Cu/Fe ions using DFT/B3LYP approach*. *Int. J. Miner. Process.*, 140, 43-49.
- DRZYMALA J., FUETSTENAN D.W., 1981. *Selective Flocculation of Hematite in the Hematite-Quartz-Ferric Ion-Polyacrylic Acid System, Part I, Activation and Deactivation of Quartz*. *Int. J. Miner. Process.*, 7, 258.
- FENG B., LUO X.P., WANG J.Q., WANG P.C., 2015. *The flotation separation of scheelite from calcite using acidified sodium silicate as depressant*. *Miner. Eng.*, 80, 45-49.
- GAO Y.S., GAO Z.Y., SUN W., HU Y.H., 2016. *Selective flotation of scheelite from calcite\_ A novel reagent scheme*. *Int. J. Miner. Process.*, 154, 10-15.

- GAO Z.W., ZHENG C.H., ZHANG Z.R., XIN B.J., 2010. *Experimental Study of Scheelite Flotation at Room Temperature*, China Tungsten Ind., 25(6), 18-20. (in Chinese)
- GAO Z.Y., SUN W., HU Y.H., 2013, *Surface energies and appearances of commonly exposed surface of scheelite crystal*. Trans. Nonferrous Met. Soc. China, 23 (7), 2147-2152.
- GAO Z.Y., SUN W., HU Y.H., 2015. *New insights into the dodecylamine adsorption on scheelite and calcite: An adsorption model*. Miner. Eng., 79(2015), 54-61.
- GAO Z.Y., BAI D., SUN W., CAO X.F., HU Y.H., 2015, *Selective flotation of scheelite from calcite and fluorite using a collector mixture*, Miner. Eng., 72, 23-26.
- GUERRERO L., OMIL F., MENDEZ, LEMA R. J. M., 1998. *Protein recovery during the overall treatment of wastewaters from fish-meal factories*. Biores. Technol., 63(3), 221-229.
- HU H.P., WANG M., DING Z.Y., JI G.F., 2016. *FT-IR, XPS and DFT Study of the Adsorption Mechanism of Sodium Salicylate onto Goethite or Hematite*. Acta. Phys. Chim, 32, 2059-2068.
- HU Y.H., GAO Z.Y., SUN W., LIU X.W. 2012. *Anisotropic surface energies and adsorption behaviors of scheelite crystal*. Colloids Surf. A, 415, 439-448.
- HUANG C.B., ZHANG L., WANG Y.H., LAN Y., 2008. *Separation of aluminosilicates and diasporite from diasporic-bauxite by selective flocculation*. J. Cent. S. Univ. Technol. (English Edition), 15(4), 520-525.
- KOHL P.T.L., ANDREWS J.R.G., UHLHERR P.H.T., 1986. *Floc-size distribution of scheelite treated by shear-flocculation*. Int. J. Miner. Process., 17(1-2), 45-65.
- LEEUW N. H. de and COOPER T. G., 2003. *The layering effect of water on the structure of scheelite*. Phys. Chem. Chem. Phys., 5, 433-436.
- LII Y.X., LI C.G., 1983. *Selective flotation of scheelite from calcium minerals with sodium oleate as a collector and phosphates as modifiers. I. Selective flotation of scheelite*. Int. J. Miner. Process., 10(3), 205-218.
- LIU C., FENG Q.M., ZHANG G.F., 2016. *Effect of depressants in the selective flotation of scheelite and calcite using oxidized paraffin soap as collector*. Int. J. Miner. Process., 157, 210-215.
- LIU H.W., XU Z.G., 2013. *Technical Research on Flotation of the Low-grade Scheelite at Normal Temperature by Lime-based Method*. Multipurpose Utilization of Mineral Resources, (2), 33-35 (in Chinese).
- MOREIRA G.F., PECANHA E.R., MONTE M.B.M., FILHO L.S.L., STAVALE F., 2017. *XPS study on the mechanism of starch-hematite surface chemical complexation*. Miner. Eng., 110(15), 96-103.
- PARASYUK O.V., KHYZHUN O.Y., PIASECKI M., KITYK I.V., LAKSHMINARAYANA G., LUZHNYI I., FOCHUK P.M., FEDORCHUK A.O., LEVKOVETS S.I., YRUCHENKO O.M., PISKACH L.V., 2017. *Synthesis, structural, X-ray photoelectron spectroscopy (XPS) studies and IR induced anisotropy of Tl<sub>4</sub>HgI<sub>6</sub> single crystals*. Mat. Chem. Phys., 187, 156-163.
- PAYNE M.C., TETER M.P., ALLAN D.C., ARIAS T.A., JOANNOPOULOS J.D., 1992. *Iterative minimization techniques for abinitio total-energy calculations: Molecular dynamics and conjugate gradients*. Rev. Modern Phys., 64(4), 1045-1097.
- PERDEW J.P., BURE K., ERNZERHOF M., 1996. *Generalized gradient approximation made simple*. Phys. Rev. Lett., 77(18), 3865-3868.
- PRADIP, RAI B., RAO T.K., KRISHNAMURTHY S., VETRIVEL R., MIELCZARSKI J., CASES J.M., 2002. *Molecular modelling of interactions of diphosphonic acid based surfactants with calcium minerals*. Langmuir, 18(3), 932-940.
- QIU G.Z., 1987. *The innovation of the theory and technology on the flotation of fine particles*. Changsha: Central South University of Technology (in Chinese).
- RUBIO J., MARABINI A.M., 1987, *Factors affecting the selective flocculation of hydroxyl apatite from quartz and/or calcite mixtures*, Int. J. Miner. Process., 20(1-2), 59-71.
- SILVESTRE M.O., PEREIRA C.A., GALERY R., PERES A.E.C., *Dispersion effect on a lead-zinc sulphide ore flotation*, Miner. Eng., 22(9-10), 752-758.
- SUN W., TANG H.H., CHEN C., 2013. *Solution chemistry behaviour of sodium silicate in flotation of fluorite and scheelite*, Chin. J. Nonferrous Met., 23 (8), 2274-2283.
- WANG D.Z., HU Y.H., 1988. *Solution chemistry of flotation*. Hunan Science and Technology Press. (in Chinese)
- WANG Y.H., HUANG C.B., HU Y.H., HU Y.M., LAN Y., 2008. *Beneficiation of diasporic-bauxite ore by selective flocculation with a polyacrylate flocculant*, Miner. Eng., 21(9), 664-672.
- YANG X.L., LIU S. LIU G.Y., ZHONG H., 2017. *A DFT study on the structure-reactivity relationship of aliphatic oxime derivatives as copper chelating agents and malachite flotation collectors*. J. Ind. Eng. Chem., 46, 404-415.

- YANG X.W., SHENG J.H., DA C.S., WANG H.S., WU S. , Wang Rui-Chan, Albert S. C., 2000. *Polymer-Supported BINOL Ligand for the Titanium-Catalyzed Diethylzinc Addition to Aldehydes: A Remarkable Positive Influence of the Support on the Enantioselectivity of the Catalyst*. *Journal of Organic Chemistry*, 65(2): 295-296.
- YIN W.Z., WANG J.Z., SUN Z.M., 2015. *Structure-activity relationship and mechanisms of reagents used in scheelite flotation*. *Rare Met.*, 34(12), 882-887.
- YLIKANTOLA A., LINNANTO J., KNUUTINEN J., ORAVILAHTI A., TOIVAKKA M., 2013. *Molecular modeling studies of interactions between sodium polyacrylate polymer and calcite surface*. *Appl. Surf. Sci.*, 276, 43-52.
- ZHANG Y., WANG Y.H., HU Y.H., WEN S.M., WANG J.M., 2014. *First-Principle Theory Calculation of Electronic Structures of Scheelite, Fluorite and Calcite*. *Chin. J. Rare Met.*, 38(6), 1106-1113.
- ZHAO G., ZHONG H., QIU X.Y., WANG S., GAO Y.D., DAI Z.L., HUANG J.P., LIU G.Y., 2013. *The DFT study of cyclohexyl hydroxamic acid as a collector in scheelite flotation*. *Miner. Eng.*, 49, 54-60.